ACS OMEGA

Open Access

This article is licensed under CC-BY-NC-ND 4.0

http://pubs.acs.org/journal/acsodf

Article

Silver-Catalyzed Cascade Approach to Access Fused Pyrazolo-naphthyridine and -isoquinoline Backbones and Investigation of Their Photophysical Properties

Fatemeh Abdiyan Mobarakeh, Mohammad Rezaei-Gohar, Kamran Amiri, Hamid Reza Bijanzadeh, Frank Rominger, and Saeed Balalaie*

Cite This: *ACS Omega* 2025, 10, 14063−14074

Read Online

ACCESS | Metrics & More | Article Recommendations | Supporting Information

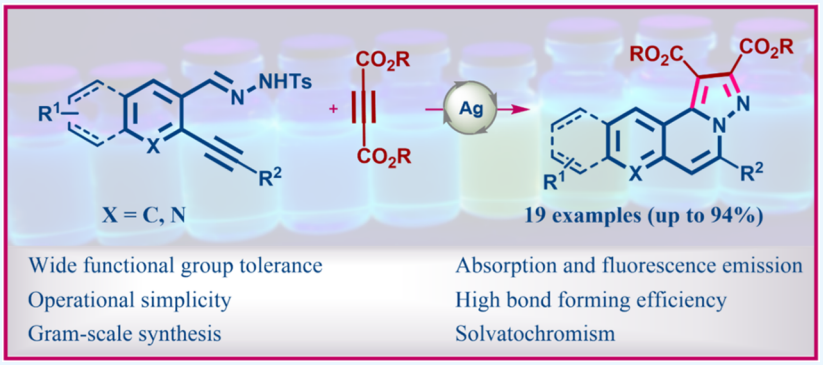

ABSTRACT: We describe a novel approach for synthesizing diverse fused heterocyclic compounds by utilizing a sequential silver(I) catalyzed reaction between readily obtainable *N*-amidonaphthyridin ylide and dialkyl acetylenedicarboxylates. This method provides an efficient approach for the selective synthesis of tetracyclic ring-fused 1,6-naphthyridine and isoquinoline derivatives, offering exceptional structural diversity. In addition, the title compounds constitute an interesting class of luminophores with tunable emission solvatochromicity.

INTRODUCTION

N-imide ylides as zwitterionic intermediates with octet structures are remarkable motifs of organic building blocks utilized for the construction of nitrogen-containing biologically active compounds.[1] The appeal of bifunctional reagents arises from their capacity to exhibit dual reactivity modes.[2] *N*-imide ylides exhibit diverse reactivity modes and can participate in a broad spectrum of reactions, including C−H functionalization, nucleophilic addition, and cycloaddition.[3] The cycloaddition reaction of *N*-imide ylides provides an efficient pathway for the synthesis of *N*-heterocyclic scaffolds.[4] These privileged structures serve as versatile platforms for the construction of complex natural products, thus facilitating the discovery of novel bioactive molecules with therapeutic potential.[5,6] It should be noted that recent investigations indicate that nitrogen-containing heterocycles are prevalent within the structures of >90% of drug candidates currently under development by pharmaceutical companies. Among these, pyridines and their derivatives, namely, particularly valuable 1,6-naphthyridines, emerge as the most prominent family within this domain.[7]

Pyrazolopyridines and their extended derivatives, including pyrazolo-1,6-naphthopyridines, form a cohesive family of heterocyclic compounds. The synthesis of pyrazolopyridines has become a central thrust in modern organic synthesis due to their prevalence in bioactive natural products and pharmaceuticals. This class of pyrazolopyridine and diverse pyrazolo-1,6-naphthopyridine scaffolds is found widely in both drugs and biological molecules and include CB2 receptor antagonists (inverse agonists),[8a] dopamine D3 agonists (the treatment of psychostimulant addictions),[8b] $5HT_3$-adenosine antagonists (nicotinic acetylcholine, glycine, and $GABA_A$ receptors/the treatment of emesis and irritable bowel syndrome),[8c] and adenosine A1 receptor antagonist (the treatment of cardiac arrhythmias and for the diagnosis of ischemic heart diseases),[8d] as illustrated in Figure 1.

Nevertheless, in view of their potential applications, core-containing scaffolds are very rare. Consequently, the development of efficient synthetic methodologies to access these

Received: December 9, 2024
Revised: February 11, 2025
Accepted: February 26, 2025
Published: April 4, 2025

© 2025 The Authors. Published by American Chemical Society

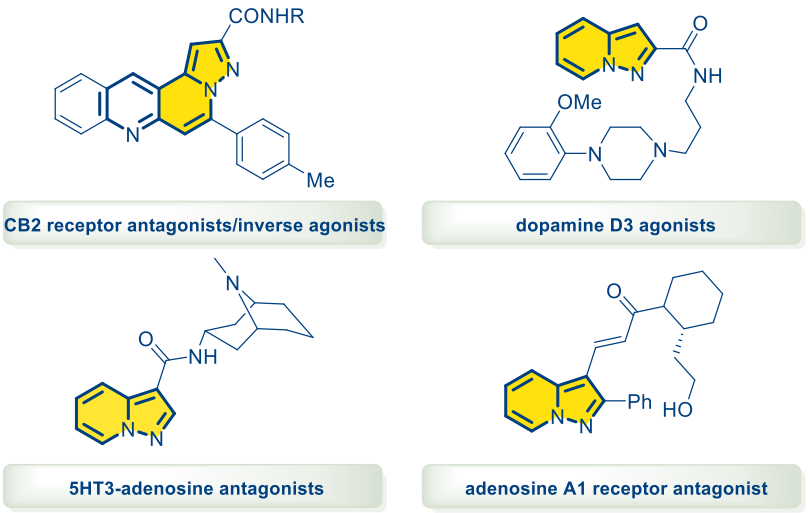

Figure 1. Selected examples of biologically active pyrazolopyridines and pyrazolo-1,6-naphthyridine derivatives.

valuable frameworks has become a topic of significant interest. To the best of our knowledge, some previous studies, as illustrated in Scheme 1a–e, have reported cycloaddition reactions between *N*-amidoisoquinolinium ylides and a diverse array of substrates.

These reactions, including those involving 2-alkylenecyclobutanone (Scheme 1a),[9] bromoalkynes and alkenyl iodide (Scheme 1b,c),[10] 3-phenylpropiolaldehyde (Scheme 1d),[11] *α,β*-unsaturated aldehydes (Scheme 1e),[12] have emerged as efficient strategies for the synthesis of substituted pyrazolopyridines structures as five-membered *N*-heterocyclic frameworks. The aforementioned four examples of existing methods for synthesizing these scaffolds face significant challenges, such as the need for harsh conditions, lengthy multistep procedures, costly reagents, and/or dependence on hazardous dual-transition-metal catalysis. In this regard, promoting a new synthetic strategy that enables one-step procedures, thereby eliminating the need for multistep processes, is in high demand. The synthetic strategic utilization of bifunctional reagents, harboring both nucleophilic and latent radical character, offers a powerful approach for the streamlined synthesis of complex molecular architectures.[13] These versatile reagents exploit their inherent orthogonality reactivities within a single molecule through exploitation, enabling an efficient construction process. Therefore, we disclose the development of a highly efficient one-step method for the synthesis of pyrazolo-naphthyridine and pyrazolo-isoquinoline derivatives, utilizing novel *N*-imide ylides as key intermediates. This approach enables the production of functionalized fused heterocyclic compounds with exceptional efficiency and minimal catalyst loading. The reaction could proceed through *in situ* formation of imide ylide as a 1,3-dipole from and its [3 + 2] cycloaddition reaction with dialkyl acetylenedicarboxylates catalyzed by Ag(I).

RESULTS AND DISCUSSION

At the outset, we investigated the optimal reaction conditions to achieve the synthesis of compound **3a**. We employed model substrates, *N*′-(2-alkynylquinolinylmethylene)hydrazide (**1a**) and diethyl acetylenedicarboxylates (**2a**), to identify the ideal suitable reaction conditions. This optimization process entailed evaluating the influence of diverse catalysts, solvents, and temperatures on the behavior of model substrates (Table 1). During our initial research, the absence of a catalyst prevented product formation (Table 1, entry 1). Consequently, to enhance the reaction's efficiency, various transition-metal catalysts, including $Er(OTf)_3$, $InCl_3$, $CuCl_2$, $ZnCl_2$, $Sc(OTf)_3$, and $AgNO_3$, were evaluated, and the results revealed that employing a catalyst was found to be a requirement to achieve the desired product (Table 1, entries 2–7). It became evident that the source of silver was paramount for facilitating the proceeding, as it significantly increased the reaction yield to 82%. Following elucidation of the importance of the silver source, we evaluated the influence of various silver salt catalysts, such as $AgNO_3$, AgO_2, $AgCO_3$, AgOAc, and AgOTf. Our investigation revealed that AgOTf emerged as the most effective catalyst for the reaction, affording product **3a** in 94% yield (Table 1, entries 8–11). Subsequently, a screening of various types of polar and nonpolar solvents, including methanol (MeOH), ethanol (EtOH), trifluoroethanol (TFE), acetonitrile (CH_3CN), 1,2-dichloroethane (DCE), 1,4-dioxane, toluene, dimethylformamide (DMF), tetrahydrofuran (THF), and water, was conducted. Among these, this evaluation identified methanol as the suitable solvent to access the desired product in high yields (Table 1, entries 12–20). Moreover, our investigation established a dependence of the reaction yield on the catalyst equivalent. However, variations in the catalyst quantity did not significantly affect the yield of the desired product (Table 1, entries 21–23). Furthermore, the reaction temperature demonstrated a demonstrable effect on the yield of the desired product. Reducing the reaction temperature from 80 to 50 °C and room temperature resulted in a significant decrease, affording 60% and 18% yields, respectively. On the other hand, raising the temperature to 100 °C affords the product in 64% yield (Table 1, entries 24–26). Finally, we investigated the reaction at various time intervals and found that reducing the reaction time prevents complete conversion with the starting materials still present in the mixture and leads to a decrease in efficiency. Conversely, extending the reaction time beyond 12 h does not improve the efficiency, which remains constant.

Now that we have established the optimal reaction conditions (Table 1, entry 11), we sought to screen the substrate scope to assess the corresponding products.

Additionally, we investigated both the limitations and the generality of the protocol.

https://doi.org/10.1021/acsomega.4c11109
ACS Omega 2025, 10, 14063−14074

Scheme 1. [3 + 2] Cycloaddition Reactions, Reported in (a−e) Previous Works and the Present Work, between *N*-imide Ylides and a Diverse Array of Substrates

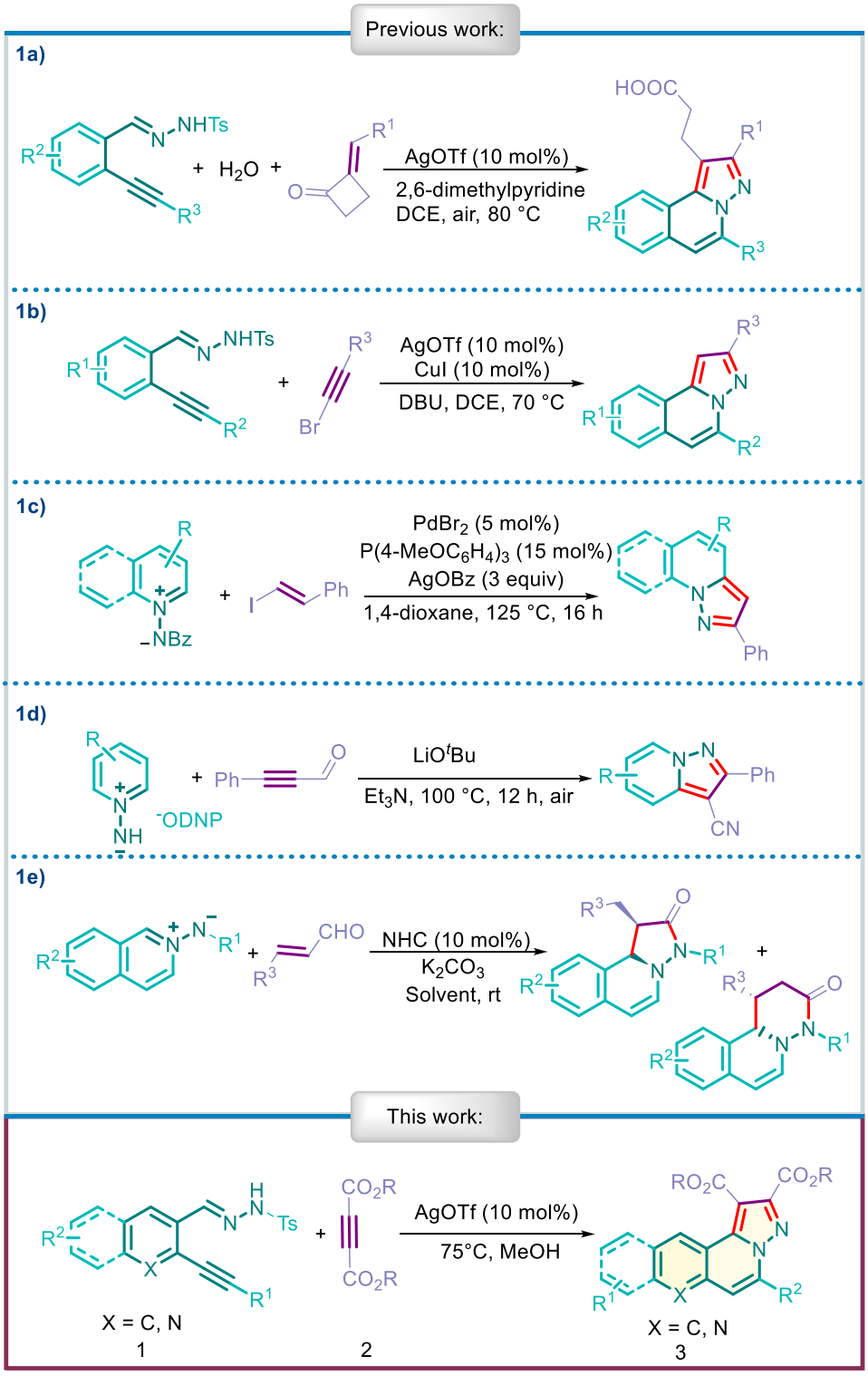

First, this study aimed to evaluate the influence of various dialkyl acetylenedicarboxylate types to determine their effect on the reaction process. Notably, despite employing diverse dialkyl acetylenedicarboxylate precursors, our findings revealed no significant changes in the product yields (Scheme 2).

Following the results achieved in detail, we introduced a broad range of substrates bearing various functional groups on the arene rings of the quinoline moiety. These substrates incorporated various functional groups, including electron-donating groups (such as isopropyl and methyl) and halogen atoms (−Cl), at four different positions on the quinoline or isoquinoline core (R^1) and participated successfully in the reaction, affording the desired products with enhanced efficiency. To investigate the influence of electron-withdrawing

https://doi.org/10.1021/acsomega.4c11109
ACS Omega 2025, 10, 14063−14074

Table 1. Optimization of the Reaction Conditions[a]

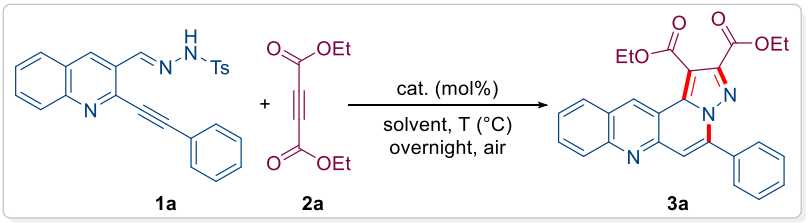

entry	cat. (mol %)	solvent	T (°C)	yield (%)[b]
1		MeOH	75	trace
2	$InCl_3$ (10)	MeOH	75	32
3	$Sc(OTf)_3$ (10)	MeOH	75	56
4	$Er(OTf)_3$ (10)	MeOH	75	43
5	$ZnCl_2$ (10)	MeOH	75	35
6	$CuCl_2$ (10)	MeOH	75	68
7	$AgNO_3$ (10)	MeOH	75	82
8	Ag_2O (10)	MeOH	75	74
9	Ag_2CO_3(10)	MeOH	75	77
10	AgOAc (10)	MeOH	75	87
11[c]	**AgOTf (10)**	**MeOH**	**75**	**94**
12	AgOTf (10)	CH_3CN	75	81
13	AgOTf (10)	DCE	75	52
14	AgOTf (10)	1,4-dioxane	75	43
15	AgOTf (10)	EtOH	75	84
16	AgOTf (10)	TFE	75	77
17	AgOTf (10)	Toluene	75	53
18	AgOTf (10)	DMF	75	59
19	AgOTf (10)	THF	75	54
20	AgOTf (10)	H_2O	75	NR
21	AgOTf (5)	MeOH	75	70
22	AgOTf (15)	MeOH	75	58
23	AgOTf (20)	MeOH	75	47
24	AgOTf (10)	MeOH	rt	18
25	AgOTf (10)	MeOH	55	60
26	AgOTf (10)	MeOH	90	64

[a]Reaction conditions: **1a** (0.2 mmol), **2a** (0.2 mmol), and catalyst (mol %) in 1.0 mL of solvent. [b]Isolated yields. [c]Within 6 h, a 50% yield is observed. This increases to 94% after 12 h of reaction time, and extending the reaction time beyond 12 h does not improve the efficiency.

groups on this reaction, we conducted experiments employing substrates bearing NO_2 and CF_3 substituents on the phenyl ring. However, these reactions did not proceed efficiently beyond the Vilsmeier−Haack step, yielding only trace amounts of the desired products. This observation indicates that the presence of electron-withdrawing groups significantly hinders the reactions. Due to the extremely low yield at this step, further advancement of the reactions was not possible. Subsequently, phenylethynyl derivatives bearing electron-donating substituents (methyl and methoxy) at the R^2 position of the aryl fragment afforded the desired product in higher yields compared to those with electron-withdrawing groups (halogens such as chlorine and bromine) on the aromatic rings, which still provided the corresponding products in good to high yields.

In order to definitively elucidate the structure of compound **3r**, single-crystal X-ray analysis was employed (CCDC number 2401250); the ellipsoid probability level was 50%. To illustrate the synthetic applicability and efficiency of this approach, the protocol was implemented in a large-scale reaction step. Initially, a large-scale [3 + 2]-annulation reaction was carried out under the optimized conditions by using 7.0 mmol *N*-amidonaphthyridin ylide to generate the desired product **3d** in 72% yield. (Scheme 3).

A series of mechanistic experiments were performed to elucidate the reaction mechanism pathway. To investigate the influence of sulfonyl moiety on reactivity, the reaction between (*E*)-3-(hydrazineylidenemethyl)-2-(phenylethynyl) quinoline **1s** and diethyl acetylenedicarboxylate **2a** was conducted under optimized conditions, but the reaction did not proceed (Scheme 4a). Subsequently, the sulfonyl-protecting group was replaced with a mesyl group. Monitoring the reaction progress revealed a notable decrease in the product yield. These results indicate the pivotal role of phenyl in facilitating the departure of the leaving group via rearomatization (Scheme 4b). Based on the outcome of this observation, we believe that the sulfonyl moiety within the quinoline core plays a crucial role in facilitating the reaction.

The substantial influence of sulfonyl moiety on the formation and stability of the desired azomethine imine is a driving force contributing to the reaction's outcome. Later, to prove the efficiency of the alkynyl component in the structure of the starting material as a key segment for intermediate formation, *p*-toluenesulfonyl hydrazide was employed to react with 2-chloroquinoline-3-carbaldehyde under standard con-

https://doi.org/10.1021/acsomega.4c11109
ACS Omega 2025, 10, 14063−14074

Scheme 2. Substrate Scope: All Reactions Were Performed on a 0.2 mmol Scale under Standard Conditions

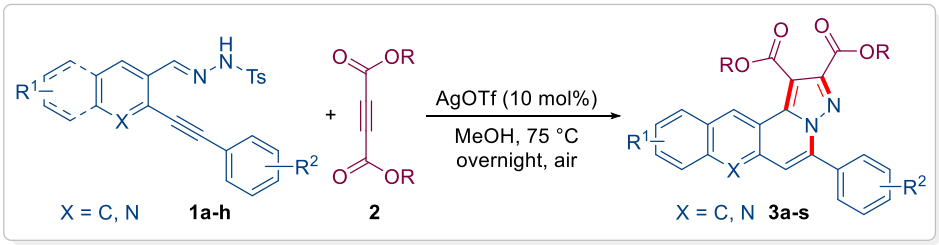

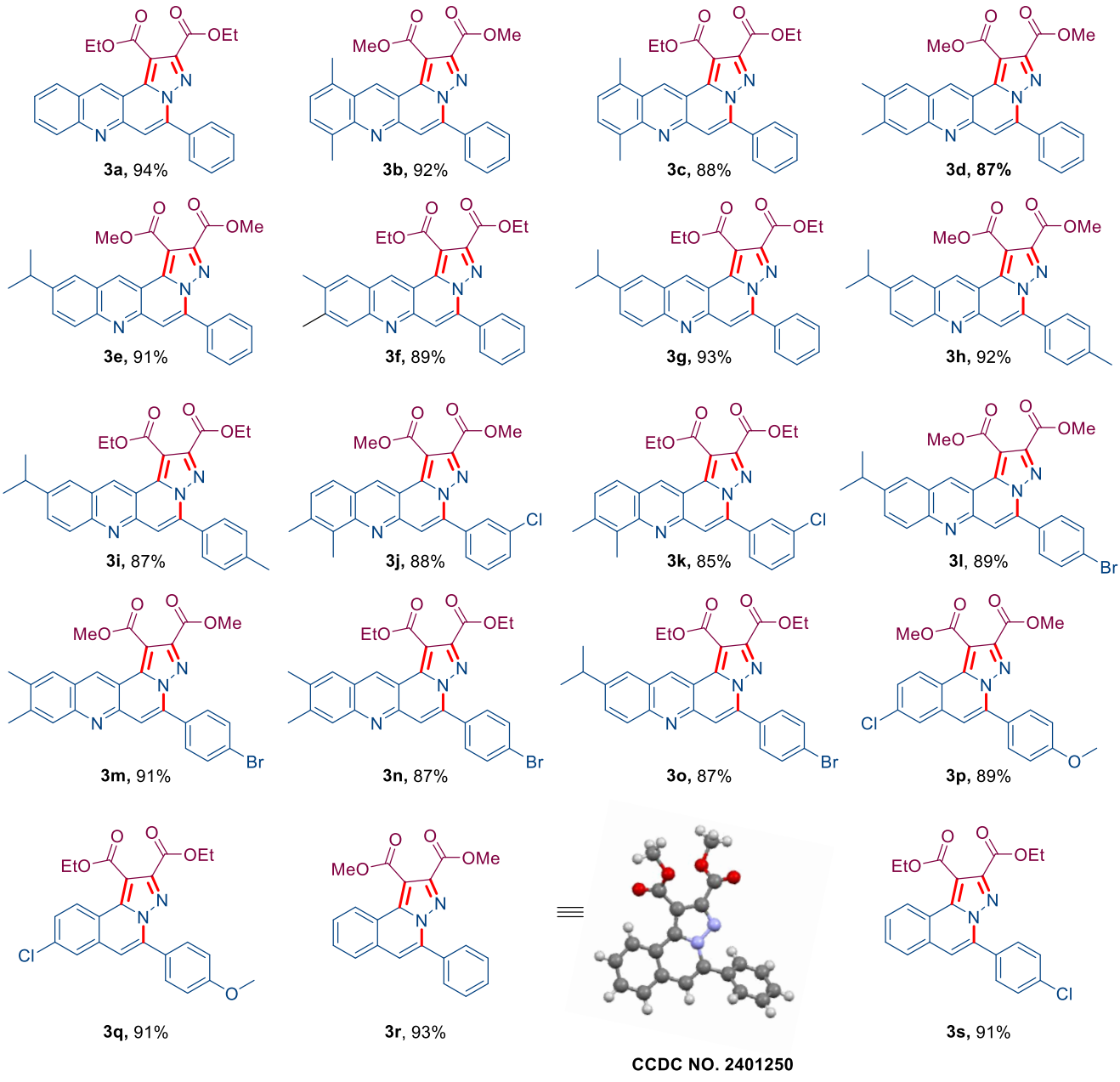

ditions (Scheme 4c). However, the anticipated product was not obtained due to inhibition of *N*-amidonaphthyridin ylide intermediate formation. This observation suggests that the phenylacetylene moiety plays a critical role in the reaction mechanism, potentially by facilitating ylide intermediate generation. In order to investigate whether silver trifluoromethanesulfonate had an essential role in the following steps after the known formation of *N*-amidonaphthyridin ylide intermediate, a control experiment was performed between independently prepared *N*-amidonaphthyridin ylide and diethyl acetylenedicarboxylate in the absence of reaction catalysis, which indicates a surprising decrease in product formation (Scheme 4d).

https://doi.org/10.1021/acsomega.4c11109
ACS Omega 2025, 10, 14063−14074

Scheme 3. Scale-up Reaction

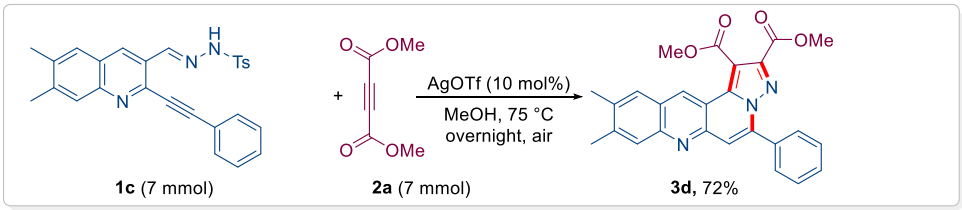

Scheme 4. (a–d) Control Experiment

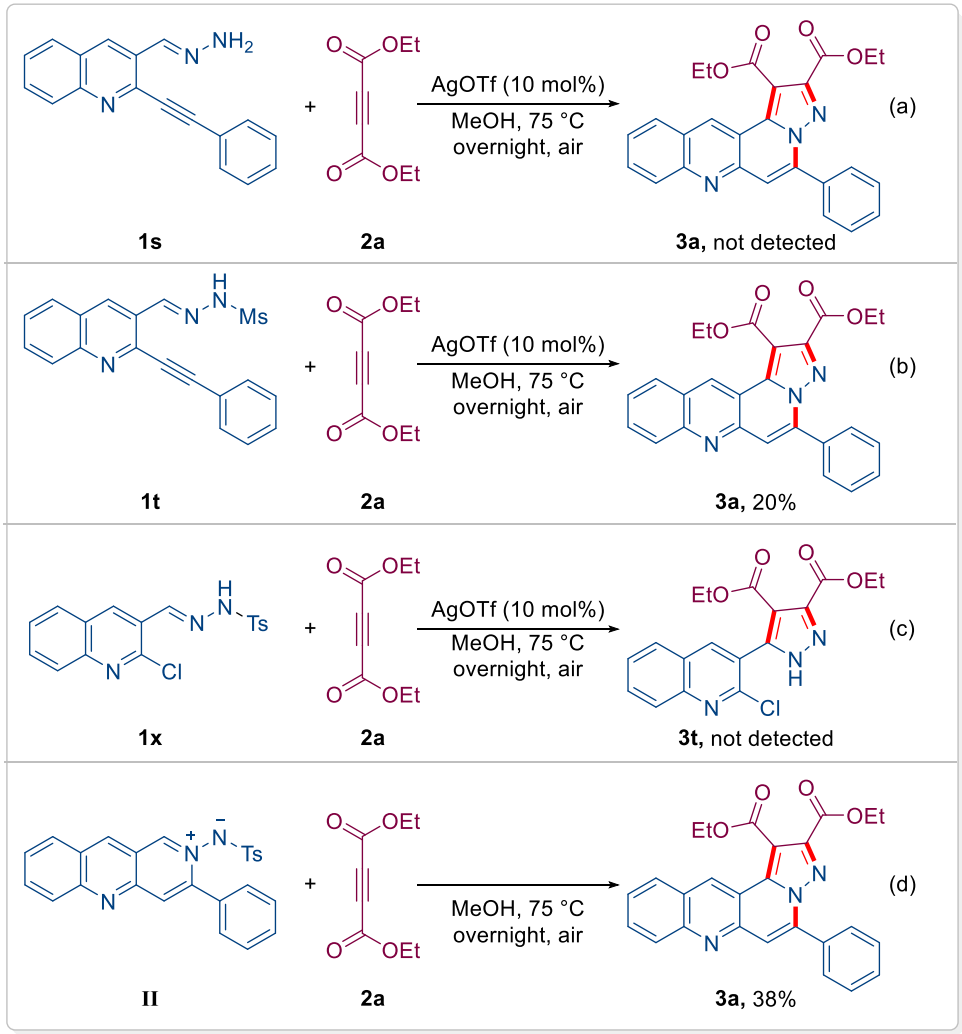

Ultimately, a possible mechanism was proposed for the synthesis of product **3**, as shown in Scheme 5.[14] Initially, this transformation is facilitated by the initiation of Ag(I)-catalysis-assisted activation of the alkyne moiety, which promotes the intramolecular nucleophilic attack by the nitrogen atom onto the alkyne moiety (**I**). Following that, a reductive elimination reaction would occur to release the silver catalyst, leading to the formation of the *N*-amidonaphthyridin ylide intermediate (**II**).

Then, the *N*-amidonaphthyridin ylide intermediate (**II**) acts as a 1,3-dipole and undergoes a 1,3-dipolar cycloaddition reaction with dialkyl acetylenedicarboxylate (**2a–b**) as the dipolarophile, resulting in the formation of the key cycloaddition intermediate **III**. Our investigations elucidated a bifunctional role of Ag(I) in the synthesis of pyrazolo-naphthyridine and isoquinoline-functionalized derivatives. Finally, intermediate **III** undergoes a dehydrogenation-desulfonylation process, which concurrently eliminates both hydrogen and the tosyl group. This step leads to aromatization of the cyclized core, affording the desired product, **3a**.

Interestingly, a significant number of pyrazolo[5,1-*f*][1,6]-naphthyridines exhibit strong luminescence in solution. To further understand this phenomenon, this study investigates the photophysical properties of a luminescent donor-π-acceptor (D-π–*A*) compound in various solvents. The absorption properties of compound **3l** were systematically examined in diverse solvent environments, including protic solvents (methanol, ethanol), polar aprotic solvents (carbon tetrachloride, 1,2-dichloroethane, chloroform, 1,4-dioxane, tetrahydrofuran, dichloromethane, dimethylformamide, di-

https://doi.org/10.1021/acsomega.4c11109
ACS Omega 2025, 10, 14063−14074

Scheme 5. Proposed Mechanism for the Synthesis of 3a−s

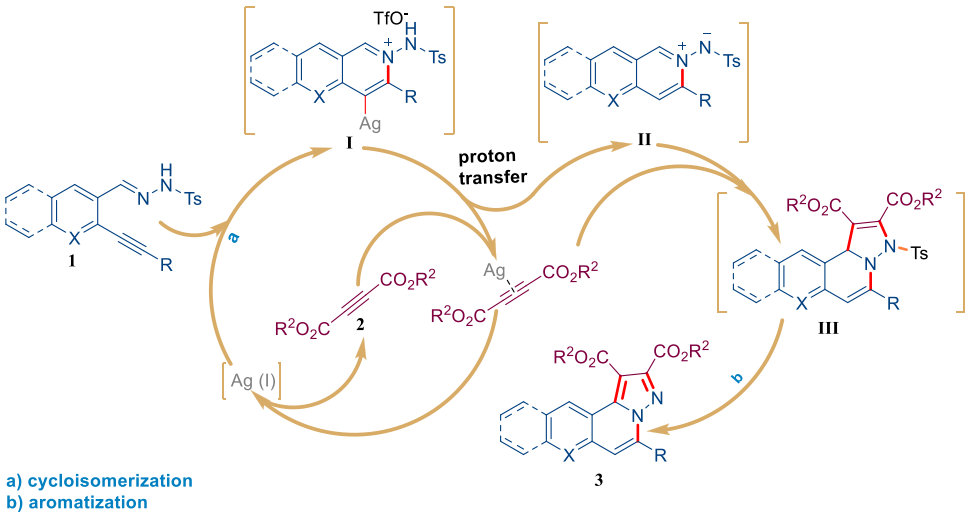

Table 2. Absorbance Data for Compound 3l in the Different Solvents

solvent	dielectric constant	λ_{abs1} (nm)	λ_{abs2} (nm)	λ_{abs3} (nm)	λ_{abs4} (nm)	ε^a ($\times 10^5$) (M^{-1} cm^{-1})	E_{gap}
CCl_4	2.24	241	300	370	392	0.41	2.97
1,4-dioxane	2.25	262	291	371	389	0.45	2.94
toluene	2.38	254	295	371	393	0.36	2.94
xylene	2.57	255	294	371	393	0.33	2.94
$CHCl_3$	4.81	266	303	370	392	0.50	2.95
THF	7.58	246	298	371	389	0.64	2.98
DCM	8.93	233	265	370	392	0.43	2.98
DCE	10.36	2221	300	370	392	0.41	2.89
EtOH	24.55	228	258	368	391	0.32	2.95
MeOH	32.70	214	294	368	391	0.30	2.95
DMF	36.70	254	275	371	392	0.40	2.90
DMSO	46.68	232	268	371	392	0.34	2.93

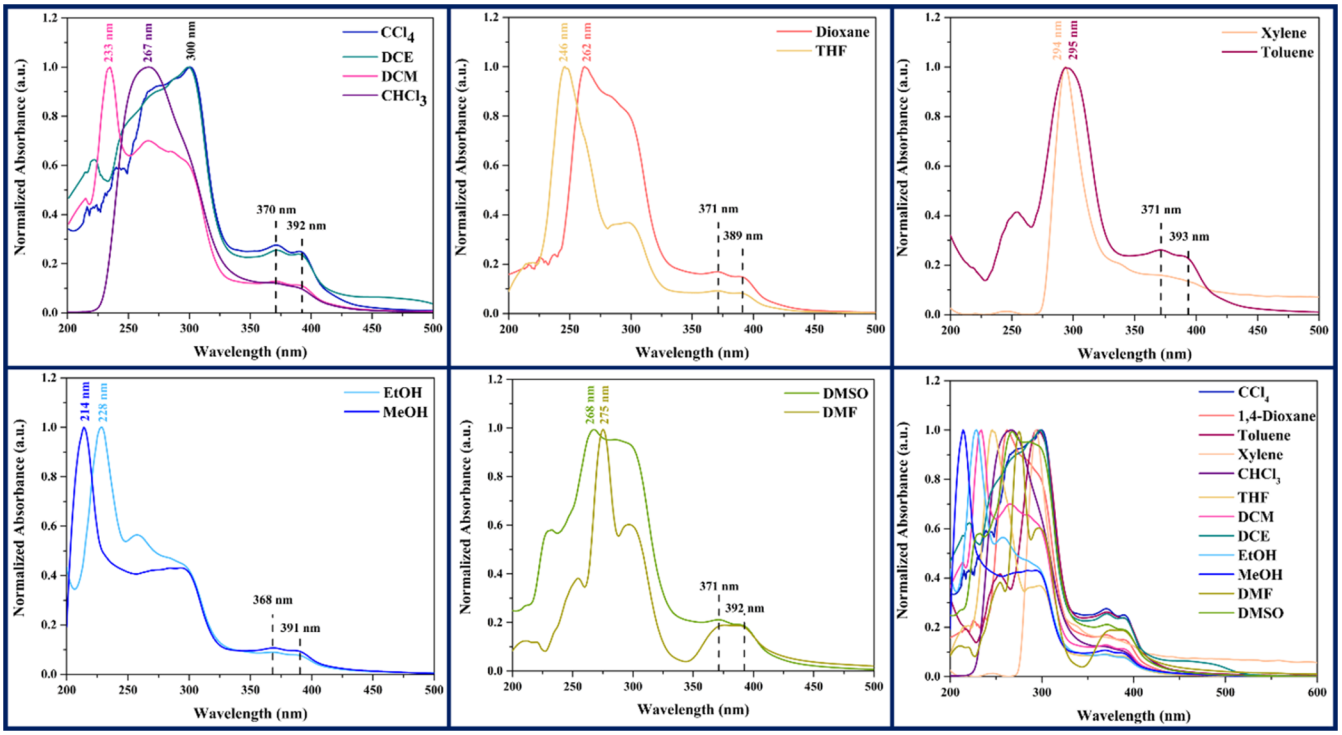

Figure 2. Absorption spectrum of compound **3l** with various solvents.

https://doi.org/10.1021/acsomega.4c11109
ACS Omega 2025, 10, 14063−14074

methyl sulfoxide), and nonpolar solvents (toluene and xylene), to assess solvent effects on its electronic transition. UV−vis absorption maxima (λ_{abs}), extinction coefficients (3), and optical band gaps (E_{gap}) are tabulated in Table 2. The UV−vis spectrum of compound **3l** (Figure 2) reveals three absorption bands. A strong absorption maximum in the range of 214−269 nm is assigned to a $\sigma-\sigma^*$ electronic transition. The second intense band, centered at around 280 nm, is attributed to a $\pi-\pi^*$ transition localized on the pyrazole moiety. Additionally, a weaker band observed at around 380 nm is assigned to an $n-\pi^*$ transition. The absorption bands of compound **3l** demonstrate a solvatochromic shift when increasing solvent polarity from 1,4-dioxane to DMSO. Protic solvents exhibited the lowest absorption bands, followed by polar aprotic solvents and finally nonpolar solvents, indicating a decrease in the energy gap.

A comparative analysis of molar extinction coefficients (ε) revealed that solvents, including THF, dioxane, and DCM, exhibited significantly higher molar extinction coefficients (ε) than polar aprotic (DMSO, DMF) and protic (EtOH, MeOH) solvents, as evidenced by the data presented in Table 2. The optical band gap (E_{gap}) for compound **3l** was determined by the absorption edge of the spectrum. The calculated E_{gap} values for the absorption band within the 417−430 nm range are tabulated in Table 3. A hypsochromic shift in the optical band gap was observed upon employing aprotic solvents such as CCl_4, 1,4-dioxane, THF, and DCM, leading to a blue shift and an increase in the E_{gap} value from 2.94 to 2.98 eV (corresponding to a wavelength shift from 417 to 421 nm). Protic solvents (MeOH, EtOH) exhibited the optical band gap energy of 2.95 eV. In contrast, polar aprotic solvents (DMF, DMSO) displayed upper band gap energies of 2.90 and 2.93 eV, respectively. These variations may be attributed to intermolecular hydrogen bonding or specific interactions involving the pyrazole moiety.

Photoluminescence (PL) spectra of compound **3l** were acquired in the same solvents used for the UV−vis absorption studies. The maximum emission wavelengths (λ_{max}) are summarized in Table 3 and graphically illustrated in Figure 3. Compound **3l** demonstrated a red shift with increasing solvent polarity. Notably, the solvent effect was more pronounced in emission than in the absorption study, resulting in a significant spectral shift from 413 to 439 nm. The optical properties of a compound can be significantly influenced by solvent polarity, resulting in substantial shifts in absorption and emission band positions and intensities. Figure 3a illustrates the significant impact of solvent polarity on the emission spectra of compound **3l**. A solvatochromic shift from green to yellowish-orange was observed upon UV irradiation. This positive solvatochromism is attributed to the stabilization of local excited states through interactions with polar solvents, resulting in a bathochromic shift.

Table 3. Emission Data Compound 3l in the Different Solvents

solvent	dielectric constant	λ_{em} (nm)
CCl_4	2.24	414
1,4-dioxane	2.25	432
toluene	2.38	429
xylene	2.57	429
$CHCl_3$	4.81	433
THF	7.58	483
DCM	8.93	432
DCE	10.36	414
EtOH	24.55	433
MeOH	32.70	439
DMF	36.70	434
DMSO	46.68	439

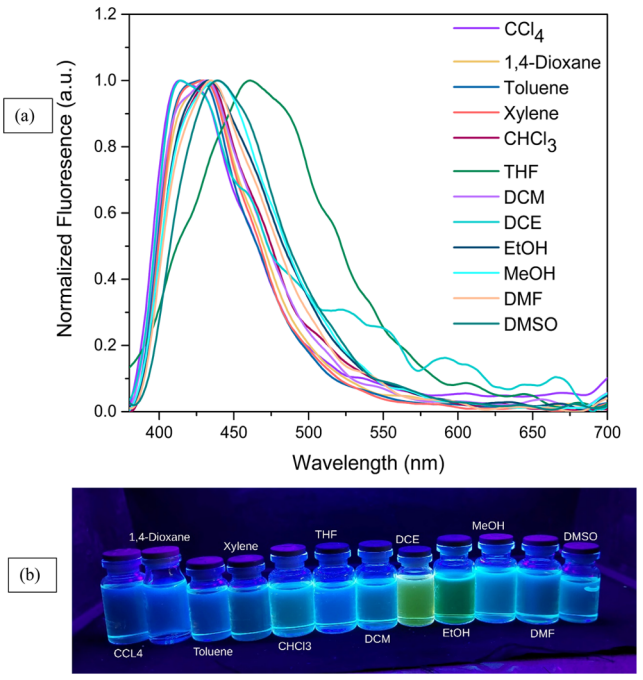

Figure 3. (a) Normalized emission spectra of compound **3l** in several solvents. (b) Solvatochromism.

CONCLUSIONS

In conclusion, we developed a general strategy for the construction of tetracyclic ring-fused 1,6-naphthyridine and isoquinoline **3a−s** as an interesting class of luminophores with tunable emission solvatochromism effects, in good to excellent yields, using two different materials, easily accessible aromatic *N*-amidonaphthyridin ylide and *N*-amidoisoquinolinium ylide. Remarkably, this reaction led to the formation of an *in situ* ylide and constructed three new bonds (C−N, C═N, and C═C) in a single step via a [3 + 2] cycloaddition reaction. Notably, this transformation was achieved through the concurrent cleavage of one C−H, one N−S, and one C−C bond. Furthermore, this methodology exhibits a broad substrate scope, excellent functional group tolerance, high efficiency, and low catalyst loading, making it a mild and operationally simple strategy. Importantly, it circumvents the limitations of existing approaches, which often require harsh reaction conditions, lengthy multistep procedures, expensive reagents, and/or reliance on hazardous dual-transition-metal catalysis. Subsequently, this gram-scale method for the synthesis of [1,6]-naphthyridines paves the way for their utilization in developing valuable bioactive compounds and pharmaceutical advancements.

EXPERIMENTAL SECTION

General Methods. All reagents and starting materials were purchased in reagent grade and used without further purification. Silica gel column chromatography was carried

https://doi.org/10.1021/acsomega.4c11109
ACS Omega 2025, 10, 14063−14074

out using Silica gel 60 (230−400 mesh). Melting points (mp) were determined in capillary tubes using an Electrothermal 9100 digital melting point apparatus and were uncorrected. Analytical thin-layer chromatography (TLC) was performed using a precoated TLC plate (silica gel 60 F_{254}) and visualized under ultraviolet (UV) light. ^{1}H and ^{13}C NMR spectra were recorded on a Bruker 250, 300, and 400 MHz spectrometer. Chemical shifts and coupling constants are reported as δ/ppm and Hz, respectively. Data are reported as follows: chemical shift, multiplicity (s = singlet, d = doublet, t = triplet, q = quartet, dd = doublet of doublets, td = triplet of doublets, m = multiplet). High-resolution mass spectra (HRMS-ESI) were attained using a Waters LCT Premier XE TOF (time-of-flight) mass spectrometer. Single-crystal X-ray data were obtained using a Bruker APEX-II Quazar area detector.

General Procedure for the Formation of Benzo[*b*]-pyrazole[5,1-*f*][1,6]naphthyridine-1,2-dicarboxylates. In a 25 mL one-necked, round-bottomed flask, the mixture of (E)-4-methyl-N′-((2-(phenylethynyl)quinolin-3-yl)-methylene)benzenesulfonohydrazide **1a−h** (0.2 mmol, 1 equiv) and silver triflate (5 mg, 10 mol %) in MeOH (1.5 mL) was stirred at 75 °C in an oil bath for about 3 h. Afterward, dialkyl acetylenedicarboxylates **2a−b** (0.2 mmol, 1 equiv) were added. The reaction mixture was stirred at 75 °C in an oil bath overnight. After completion of the reaction, as indicated by TLC, the solvent was removed under reduced pressure, and the residue was purified by column chromatography using hexane/ethyl acetate as the eluent to afford the desired benzo[*b*]pyrazole[5,1-*f*][1,6]naphthyridine-1,2-dicarboxylate products **3a−s**.

Representative Procedure for Synthesis of 3d in a Gram-Scale Reaction. In a 25 mL one-necked round-bottomed flask, the mixture of (E)-4-methyl-N′-((2-(phenylethynyl)quinolin-3-yl)methylene)-benzenesulfonohydrazide **1** (3170 mg, 7.0 mmol, 1.0 equiv) and silver triflate (187 mg, 10 mol %) in MeOH (5.3 mL) was stirred at 75 °C in an oil bath for about 3 h. Subsequently, dialkyl acetylenedicarboxylate **2a** (995 mg, 7.0 mmol, 1.0 equiv) was added. The reaction mixture was stirred at 75 °C in the oil bath overnight. After completion of the reaction, as indicated by TLC, the solvent was removed under reduced pressure, and the residue was purified by column chromatography using hexane/ethyl acetate (50:1) as the eluent to afford the desired benzo[*b*]pyrazole[5,1-*f*][1,6]naphthyridine-1,2-dicarboxylate product **3d** in 72% yield (2210 mg).

*Diethyl 5-phenylbenzo[b]pyrazolo[5,1-f][1,6]-naphthyridine-1,2-dicarboxylate (**3a**).* Yellow solid (83 mg, yield 94%, mp 190−192 °C), (*n*-hexane/EtOAc = 2:1, R_f = 0.25); **^{1}H NMR** (300 MHz, $CDCl_3$): δ_H = 9.99 (brs, 1H), 8.05 (d, *J* = 8.5 Hz, 1H), 7.96 (d, *J* = 8.3 Hz, 1H), 7.92−7.88 (m, 2H), 7.73 (t, *J* = 7.8 Hz, 1H), 7.55−7.48 (m, 5H), 4.52 (q, *J* = 7.1 Hz, 2H), 4.43 (q, *J* = 7.1 Hz, 2H), 1.46 (t, *J* = 7.1 Hz, 3H), 1.40 (t, *J* = 7.1 Hz, 3H) ppm; **$^{13}C\{^{1}H\}$ NMR** (75 MHz, $CDCl_3$): δ_C = 163.1, 162.5, 148.6, 146.3, 146.1, 141.9, 137.9, 134.3, 131.8, 131.0, 129.6, 129.4, 128.4, 128.3, 127.9, 126.2, 125.9, 116.8, 116.7, 109.4, 61.4, 61.1, 13.6 (2C) ppm; **HRMS-ESI**(+) (*m*/*z*): calcd. for $C_{26}H_{22}N_3O_4$ $[M + H]^+$ 440.1604, found 440.1605.

*Dimethyl 8,11-dimethyl-5-phenylbenzo[b]pyrazolo[5,1-f][1,6]naphthyridine-1,2-dicarboxylate (**3b**).* Yellow solid (80 mg, yield 92%, mp 180−182 °C), (*n*-hexane/EtOAc = 2:1, R_f = 0.25); **^{1}H NMR** (300 MHz, $CDCl_3$): δ_H = 10.08 (s, 1H), 7.95 (d, *J* = 7.8 Hz, 1H), 7.88−7.78 (m, 2H), 7.56 (s, 1H), 7.47−7.41 (m, 4H), 3.95 (s, 3H), 3.88 (s, 3H), 2.69 (s, 3H), 2.67 (s, 3H) ppm; **$^{13}C\{^{1}H\}$ NMR** (101 MHz, $CDCl_3$): δ_C = 164.3, 163.5, 148.9, 146.0, 145.4, 142.0, 138.9, 134.8, 133.7, 132.3, 131.1, 130.1, 129.9, 129.8, 128.5, 127.0, 126.3, 118.0, 116.5, 109.6, 52.9, 52.6, 18.9, 18.1 ppm; **HRMS-ESI**(+) (*m*/*z*): calcd. for $C_{26}H_{22}N_3O_4$ $[M + H]^+$ 440.1604, found 440.1612.

*Diethyl 8,11-dimethyl-5-phenylbenzo[b]pyrazolo[5,1-f]-[1,6]naphthyridine-1,2-dicarboxylate (**3c**).* Yellow solid (82 mg, yield 88%, mp 218−220 °C), (*n*-hexane/EtOAc = 2:1, R_f = 0.25); **^{1}H NMR** (300 MHz, $CDCl_3$): δ_H = 10.25 (s, 1H), 7.93 (brs, 2H), 7.63−7.23 (m, 6H), 4.56−4.39 (m, 4H), 2.78 (s, 6H), 1.42 (brs, 6H) ppm; **$^{13}C\{^{1}H\}$ NMR** (75 MHz, $CDCl_3$): δ_C = 163.6, 163.3, 162.7, 155.1, 148.3, 145.0, 141.5, 138.4, 134.3, 133.2, 132.0, 131.3, 130.4, 129.4, 129.3, 127.8, 126.2, 117.3, 116.1, 61.3, 61.0, 18.2, 17.3, 13.7, 13.6 ppm; **HRMS-ESI**(+) (*m*/*z*): calcd. for $C_{28}H_{26}N_3O_4$ $[M + H]^+$ 468.1917, found 468.1920.

*Dimethyl 9,10-dimethyl-5-phenylbenzo[b]pyrazolo[5,1-f][1,6]naphthyridine-1,2-dicarboxylate (**3d**).* Yellow solid (76 mg, yield 87%, mp 200−202 °C), (*n*-hexane/EtOAc = 2:1, R_f = 0.25); **^{1}H NMR** (300 MHz, $CDCl_3$): δ_H = 9.81 (brs, 1H), 7.93 (d, *J* = 3.7 Hz, 1H), 7.91 (d, *J* = 2.1 Hz, 1H), 7.89 (s, 1H), 7.76 (brs, 1H), 7.58−7.50 (m, 4H), 4.05 (s, 3H), 3.97 (s, 3H), 2.49 (s, 3H), 2.46 (s, 3H) ppm; **$^{13}C\{^{1}H\}$ NMR** (75 MHz, $CDCl_3$): δ_C = 163.8, 162.8, 145.5, 145.4, 142.5, 141.5, 138.2, 137.0, 133.0, 131.8, 129.5, 129.3, 127.9, 127.4, 127.3, 124.9, 116.8, 116.3, 109.0, 52.2, 52.0, 20.3, 19.6 ppm; **HRMS-ESI**(+) (*m*/*z*): calcd. for $C_{26}H_{22}N_3O_4$ $[M + H]^+$ 440.1604, found 440.1597.

*Dimethyl 10-isopropyl-5-phenylbenzo[b]pyrazolo[5,1-f]-[1,6]naphthyridine-1,2-dicarboxylate (**3e**).* Yellow solid (82 mg, yield 91%, mp 182−184 °C), (*n*-hexane/EtOAc = 2:1, R_f = 0.25); **^{1}H NMR** (300 MHz, $CDCl_3$): δ_H = 9.95 (brs, 1H), 8.09 (d, *J* = 8.9 Hz, 1H), 7.92 (d, *J* = 2.8 Hz, 1H), 7.91−7.89 (m, 1H), 7.89−7.83 (m, 2H), 7.75 (dd, *J* = 8.9, 1.9 Hz, 1H), 7.56 (brs, 1H), 7.52 (brs, 2H), 4.05 (s, 3H), 3.97 (s, 3H), 3.21−3.05 (m, 1H), 1.38 (d, *J* = 6.9 Hz, 3H), 1.37 (d, *J* = 6.9 Hz, 3H) ppm; **$^{13}C\{^{1}H\}$ NMR** (75 MHz, $CDCl_3$): δ_C = 163.8, 162.7, 147.9, 147.2, 145.8, 145.4, 141.6, 138.2, 133.7, 133.7, 131.8, 129.5, 129.3, 128.3, 127.9, 126.2, 124.3, 117.0, 116.9, 109.3, 52.2, 52.1, 33.7, 23.2, 23.1 ppm; **HRMS-ESI**(+) (*m*/*z*): calcd. for $C_{27}H_{24}N_3O_4$ $[M + H]^+$ 454.1761, found 454.1756.

*Diethyl 9,10-dimethyl-5-phenylbenzo[b]pyrazolo[5,1-f]-[1,6]naphthyridine-1,2-dicarboxylate (**3f**).* Yellow solid (83 mg, yield 89%, mp 244−246 °C), (*n*-hexane/EtOAc = 2:1, R_f = 0.25); **^{1}H NMR** (300 MHz, $CDCl_3$): δ_H = 9.92 (brs, 1H), 7.94 (d, *J* = 3.5 Hz, 1H), 7.91 (brs, 1H), 7.87 (brs, 1H), 7.76 (brs, 1H), 7.57−7.50 (m, 4H), 4.52 (q, *J* = 7.0 Hz, 2H), 4.45 (q, *J* = 7.5 Hz, 2H), 2.48 (s, 3H), 2.45 (s, 3H), 1.47 (t, *J* = 6.9 Hz, 3H), 1.42 (t, *J* = 6.9 Hz, 3H) ppm; **$^{13}C\{^{1}H\}$ NMR** (75 MHz, $CDCl_3$): δ_C = 163.3, 162.6, 148.1, 146.0, 145.8, 142.3, 141.4, 138.2, 136.8, 133.0, 132.9, 131.9, 129.4, 127.9, 127.4, 127.3, 124. 9, 116.9, 116.4, 108.9, 61.4, 61.0, 20.4, 20.3, 19.6, 19.5 ppm; **HRMS-ESI**(+) (*m*/*z*): calcd. for $C_{28}H_{26}N_3O_4$ $[M + H]^+$ 468.1917, found 468.1920.

*Diethyl 10-isopropyl-5-phenylbenzo[b]pyrazolo[5,1-f]-[1,6]naphthyridine-1,2-dicarboxylate (**3g**).* Yellow solid (89 mg, yield 93%, mp 250−252 °C), (*n*-hexane/EtOAc = 2:1, R_f = 0.25); **^{1}H NMR** (300 MHz, $CDCl_3$): δ_H = 10.10 (s, 1H), 8.11 (d, *J* = 8.8 Hz, 1H), 7.93 (d, *J* = 3.7 Hz, 1H), 7.91 (brs, 1H), 7.88 (brs, 1H), 7.76 (d, *J* = 8.9 Hz, 1H), 7.57 (brs, 1H), 7.56−7.42 (m, 3H), 4.53 (q, *J* = 7.3 Hz, 2H), 4.45 (q, *J* = 7.3

https://doi.org/10.1021/acsomega.4c11109
ACS Omega 2025, 10, 14063−14074

Hz, 2H), 3.19−3.05 (m, 1H), 1.46 (t, J = 8.1 Hz, 3H), 1.44−1.41 (m, 3H), 1.39 (d, J = 7.0 Hz, 6H) ppm; **^{13}C{^{1}H} NMR** (75 MHz, $CDCl_3$): δ_C = 163.3, 162.6, 147.9, 147.1, 146.2, 145.9, 141.6, 138.2, 134.0, 131.9, 131.7, 129.5, 129.3, 128.3, 127.9, 126.2, 124.3, 117.0, 116.9, 109.2, 61.4, 61.1, 33.7, 23.1 (2C), 13.6 (2C) ppm; **HRMS-ESI(+)** (m/z): calcd. for $C_{29}H_{28}N_3O_4$ [**M + H**]$^+$ 482.2074, found 482.2076.

*Dimethyl 10-isopropyl-5-(p-tolyl)benzo[b]pyrazolo[5,1-f]-[1,6]naphthyridine-1,2-dicarboxylate (**3h**).* Yellow solid (86 mg, yield 92%, mp 150−152 °C), (*n*-hexane/EtOAc = 2:1, R_f = 0.25); **^{1}H NMR** (300 MHz, $CDCl_3$): δ_H = 99.94 (s, 1H), 8.09 (d, J = 8.8 Hz, 1H), 7.86 (s, 1H), 7.82 (d, J = 7.9 Hz, 2H), 7.76 (dd, J = 8.8, 2.0 Hz, 1H), 7.55 (brs, 1H), 7.34 (d, J = 7.9 Hz, 2H), 4.06 (s, 3H), 3.97 (s, 3H), 3.20−3.05 (m, 1H), 2.45 (s, 3H), 1.38 (d, J = 6.9 Hz, 6H) ppm; **^{13}C{^{1}H} NMR** (75 MHz, $CDCl_3$): δ_C = 163.9, 162.8, 147.9, 147.1, 145.9, 145.4, 141.7, 139.7, 138.2, 133.7, 131.7, 129.2, 128.9, 128.7, 128.3, 126.1, 124.3, 116.8, 116.6, 109.2, 52.2, 52.1, 33.7, 23.2, 23.1, 21.0 ppm; **HRMS-ESI(+)** (m/z): calcd. for $C_{28}H_{26}N_3O_4$ [**M + H**]$^+$ 468.1918, found 468.1928.

*Diethyl 10-isopropyl-5-(p-tolyl)benzo[b]pyrazolo[5,1-f]-[1,6]naphthyridine-1,2-dicarboxylate (**3i**).* Yellow solid (86 mg, yield 87%, mp 240−242 °C), (*n*-hexane/EtOAc = 2:1, R_f = 0.25); **^{1}H NMR** (300 MHz, $CDCl_3$): δ_H = 10.12 (brs, 1H), 8.12 (d, J = 8.8 Hz, 1H), 7.89 (s, 1H), 7.83 (d, J = 7.8 Hz, 2H), 7.79 (dd, J = 8.9, 1.9 Hz, 1H), 7.58 (brs, 1H), 7.35 (d, J = 7.8 Hz, 2H), 4.53 (q, J = 7.1 Hz, 2H), 4.45 (q, J = 7.1 Hz, 2H), 3.23−3.06 (m, 1H), 2.46 (s, 3H), 1.49−1.42 (m, 6H), 1.40 (d, J = 6.9 Hz, 6H) ppm; **^{13}C{^{1}H} NMR** (75 MHz, $CDCl_3$): δ_C = 163.3, 162.6, 148.0, 147.1, 146.1, 146.0, 141.8, 139.7, 138.2, 133.9, 131.7, 129.2, 129.0, 128.6, 128.3, 126.2, 124.3, 117.0, 116.5, 109.2, 61.4, 61.1, 33.7, 23.2, 20.9, 13.7, 13.6 ppm; **HRMS-ESI(+)** (m/z): calcd. for $C_{30}H_{30}N_3O_4$ [**M + H**]$^+$ 496.2230, found 496.2227.

*Dimethyl 5-(3-chlorophenyl)-8,9-dimethylbenzo[b]-pyrazolo[5,1-f][1,6]naphthyridine-1,2-dicarboxylate(**3j**).* Yellow solid (79 mg, yield 88%, mp 148−150 °C), (*n*-hexane/EtOAc = 2:1, R_f = 0.25); **^{1}H NMR** (500 MHz, $CDCl_3$): δ_H = 9.83 (brs, 1H), 7.92 (t, J = 1.8 Hz, 1H), 7.83 (dt, J = 7.2, 1.7 Hz, 1H), 7.79 (d, J = 8.5 Hz, 1H), 7.59 (d, J = 0.9 Hz 1H), 7.50 (t, J = 1.8 Hz, 1H), 7.49 (d, J = 7.4 Hz, 1H), 7.42 (d, J = 8.4 Hz, 1H), 4.06 (s, 3H), 4.00 (s, 3H), 2.81 (s, 3H), 2.54 (s, 3H) ppm; **^{13}C{^{1}H} NMR** (126 MHz, $CDCl_3$): δ_C = 164.1, 163.2, 148.4, 145.9, 145. 6, 140.1, 139.5, 138.8, 134.5, 134.4, 134.0, 133.9, 130.4, 130.0, 129.8, 129.6, 128.0, 125.9, 125.0, 118.7, 116.2, 109.5, 52.8, 52.6, 20.9, 13.2 ppm; **HRMS-ESI(+)** (m/z): calcd. for $C_{26}H_{21}{}^{35}ClN_3O_4$ [**M + H**]$^+$ 474.1215, found 474.1224.

*Diethyl 5-(3-chlorophenyl)-8,9-dimethylbenzo[b]-pyrazolo[5,1-f][1,6]naphthyridine-1,2-dicarboxylate (**3k**).* Yellow solid (85 mg, yield 85%, mp 205−207 °C), (*n*-hexane/EtOAc = 2:1, R_f = 0.25); **^{1}H NMR** (500 MHz, $CDCl_3$): δ_H = 10.00 (brs, 1H), 7.94 (t, J = 2.0 Hz, 1H), 7.86−7.82 (m, 3H), 7.62 (brs, 1H), 7.49 (d, J = 7.4 Hz, 1H), 7.45 (d, J = 8.6 Hz, 1H), 4.54 (q, J = 7.1 Hz, 2H), 4.45 (q, J = 7.1 Hz, 2H), 2.84 (s, 3H), 2.57 (s, 3H), 1.49 (t, J = 7.1 Hz, 3H), 1.45 (t, J = 7.1 Hz, 3H) ppm; **^{13}C{^{1}H} NMR** (126 MHz, $CDCl_3$): δ_C = 163.6, 163.0, 148.5, 146.6, 145.7, 140.2, 139.5, 138.8, 134.8, 134.3, 134.1, 134.0, 130.4, 130.0, 129.8, 129.6, 128.1, 125.9, 125.2, 118.5, 116.4, 109.5, 62.0, 61.6, 20.9 (2C), 14.2, 14.2, 14.1 ppm; **HRMS-ESI(+)** (m/z): calcd. for $C_{28}H_{25}{}^{35}ClN_3O_4$ [**M + H**]$^+$ 502.1527, found 502.1525.

*Dimethyl 5-(4-bromophenyl)-10-isopropylbenzo[b]-pyrazolo[5,1-f][1,6]naphthyridine-1,2-dicarboxylate (**3l**).* Yellow solid (94 mg, yield 89%, mp 180−182 °C), (*n*-hexane/EtOAc = 2:1, R_f = 0.25); **^{1}H NMR** (300 MHz, $CDCl_3$): δ_H = 9.99 (brs, 1H), 8.14 (d, J = 8.9 Hz, 1H), 7.90 (brs, 1H), 7.81 (d, J = 8.2 Hz, 2H), 7.79 (brs, 1H), 7.69 (d, J = 8.2 Hz, 2H), 7.60 (brs, 1H), 4.07 (s, 3H), 3.99 (s, 3H), 3.22−3.16 (m, 1H), 1.41 (d, J = 6.8 Hz, 6H) ppm; **^{13}C{^{1}H} NMR** (101 MHz, $CDCl_3$): δ_C = 164.3, 163.2, 148.5, 148.0, 146.0, 145.9, 140.9, 138.7, 134.3, 133.8, 132.5, 131.8, 131.3, 131.1, 128.8, 126.8, 124.8, 117.6, 117.4, 109.9, 52.9, 52.8, 34.3, 23.7 ppm; **HRMS-ESI(+)** (m/z): calcd. $C_{27}H_{23}{}^{79}BrN_3O_4$ [**M + H**]$^+$ 532.0866, found 532.0864.

*Dimethyl 5-(4-bromophenyl)-9,10-dimethylbenzo[b]-pyrazolo[5,1-f][1,6]naphthyridine-1,2-dicarboxylate (**3m**).* Yellow solid (94 mg, yield 91%, mp 207−209 °C), (*n*-hexane/EtOAc = 2:1, R_f = 0.25); **^{1}H NMR** (500 MHz, $CDCl_3$): δ_H = 9.84 (brs, 1H), 7.91 (s, 1H), 7.82 (s, 1H), 7.81 (d, J = 8.3 Hz, 2H), 7.68 (d, J = 8.3 Hz, 2H), 7.54 (s, 1H), 4.07 (s, 3H), 4.00 (s, 3H), 2.53 (s, 3H), 2.50 (s, 3H) ppm; **^{13}C{^{1}H} NMR** (126 MHz, $CDCl_3$): δ_C = 164.2, 163.2, 148.7, 145.9, 145.8, 143.1, 140.6, 138.8, 137.6, 133.3, 131.7, 131.3, 131.1, 127.9, 127.8, 125.5, 124.5, 117.6, 116.8, 109.6, 52.8, 52.6, 20.8, 20.1 ppm; **HRMS-ESI(+)** (m/z): calcd. for $C_{26}H_{21}{}^{79}BrN_3O_4$ [**M + H**]$^+$ 518.0709, found 518.0714.

*Diethyl 5-(4-bromophenyl)-9,10-dimethylbenzo[b]-pyrazolo[5,1-f][1,6]naphthyridine-1,2-dicarboxylate (**3n**).* Yellow solid (95 mg, yield 87%, mp 220−222 °C), (*n*-hexane/EtOAc = 2:1, R_f = 0.25); **^{1}H NMR** (500 MHz, $CDCl_3$): δ_H = 9.94 (brs, 1H), 7.90 (s, 1H), 7.81 (q, J = 8.5 Hz, 2H), 7.80 (s, 1H), 7.68(d, J = 8.5 Hz, 2H), 7.52 (s, 1H), 4.54 (q, J = 7.1 Hz, 2H), 4.47 (q, J = 7.1 Hz, 2H), 2.51 (s, 3H), 2.49 (s, 3H), 1.48 (t, J = 7.1 Hz, 3H), 1.44 (t, J = 7.1 Hz, 3H) ppm; **^{13}C{^{1}H} NMR** (126 MHz, $CDCl_3$): δ_C = 163.7, 163.0, 148.6, 146.5, 146.0, 142.9, 140.6, 138.7, 137.5, 133.5, 131.6, 131.3, 131.2, 127.9, 127.8, 125.5, 124.4, 117.5, 116.9, 109.5, 62.0, 61.6, 20.8, 20.1, 14.2, 14.1 ppm; **HRMS-ESI(+)** (m/z): calcd. for $C_{28}H_{25}{}^{79}BrN_3O_4$ [**M + H**]$^+$ 546.1022, found 546.1023.

*Diethyl 5-(4-bromophenyl)-10-isopropylbenzo[b]-pyrazolo[5,1-f][1,6]naphthyridine-1,2-dicarboxylate (**3o**).* Yellow solid (97 mg, yield 87%, mp 198−200 °C), (*n*-hexane/EtOAc = 2:1, R_f = 0.25); **^{1}H NMR** (500 MHz, $CDCl_3$): δ_H = 10.11 (brs, 1H), 8.13 (d, J = 9.5 Hz, 1H), 7.90 (s, 1H), 7.88−7.77 (m, 3H), 7.68 (d, J = 8.7 Hz, 2H), 7.58 (s, 1H), 4.55 (q, J = 7.9 Hz, 2H), 4.47 (q, J = 7.9 Hz, 2H), 3.20−3.14 (m, 1H), 1.54−1.32 (m, 12H) ppm; **^{13}C{^{1}H} NMR** (126 MHz, $CDCl_3$): δ_C = 163.7, 163.0, 148.4, 147.8, 146.7, 146.1, 140.9, 138.7, 134.5, 132.4, 131.7, 131.3, 131.2, 128.8, 126.8, 124.8, 124.5, 117.5, 117.4, 109.8, 62.0, 61.7, 34.2, 23.6 (2C), 14.2, 14.1 ppm; **HRMS-ESI(+)** (m/z): calcd. for $C_{29}H_{27}{}^{79}BrN_3O_4$ [**M + H**]$^+$ 560.1179, found 560.1177.

*Dimethyl 8-chloro-5-(4-methoxyphenyl)pyrazolo[5,1-a]-isoquinoline-1,2-dicarboxylate (**3p**).* Yellow solid (75 mg, yield 89%, mp 214−216 °C), (*n*-hexane/EtOAc = 2:1, R_f = 0.25); **^{1}H NMR** (300 MHz, $CDCl_3$): δ_H = 8.90 (d, J = 8.9 Hz, 1H), 7.77 (d, J = 8.0 Hz, 2H), 7.71 (brs, 1H), 7.52 (d, J = 8.9 Hz, 1H), 7.10 (s, 1H), 7.01 (d, J = 8.3 Hz, 2H), 3.99 (s, 3H), 3.95 (s, 3H), 3.86 (s, 3H) ppm; **^{13}C{^{1}H} NMR** (75 MHz, $CDCl_3$): δ_C = 164.1, 162.8, 160.4, 144.9, 138.7, 137.8, 135.1, 131.4, 130.6, 127.7, 126.8, 125.8, 124.1, 120.9, 113.7, 113.5, 107.5, 54.9, 52.1, 52.0 ppm; **HRMS-ESI(+)** (m/z): calcd. for $C_{22}H_{18}{}^{35}ClN_2O_5$ [**M + H**]$^+$ 425.0898, found 425.0891.

https://doi.org/10.1021/acsomega.4c11109
ACS Omega 2025, 10, 14063−14074

*Diethyl 8-chloro-5-(4-methoxyphenyl)pyrazolo[5,1-a]-isoquinoline-1,2-dicarboxylate (**3q**).* Yellow solid (82 mg, yield 91%, mp 230−232 °C), (*n*-hexane/EtOAc = 2:1, R_f = 0.25); **^{1}H NMR** (300 MHz, $CDCl_3$): δ_H = 9.05 (d, *J* = 8.8 Hz, 1H), 7.79 (dd, *J* = 8.8, 1.2 Hz, 2H), 7.72 (d, *J* = 1.6 Hz, 1H), 7.54 (dd, *J* = 8.8, 1.9 Hz, 1H), 7.10 (s, 1H), 7.00 (d, *J* = 8.6 Hz, 2H), 4.47 (q, *J* = 7.2 Hz, 2H), 4.43 (q, *J* = 7.2 Hz, 2H), 3.87 (s, 3H), 1.42 (t, *J* = 7.2 Hz, 3H), 1.38 (t, *J* = 7.2 Hz, 3H) ppm; **^{13}C{^{1}H} NMR** (75 MHz, $CDCl_3$): δ_C = 163.6, 162.6, 160.4, 145.6, 138.7, 137.8, 135.0, 131.4, 130.6, 127.6, 127.1, 125.8, 124.2, 121.1, 113.6, 113.4, 107.4, 61.3, 61.0, 54.9, 13.7, 13.6 ppm; **HRMS-ESI**(+) (*m*/*z*): calcd. for $C_{24}H_{22}{}^{35}ClN_2O_5$ [**M** + **H**]$^+$ 453.1211, found 453.1204.

*Dimethyl 5-phenylpyrazolo[5,1-a]isoquinoline-1,2-dicarboxylate (**3r**).* White solid (67 mg, yield 93%, mp 175−177 °C), (*n*-hexane/EtOAc = 2:1, R_f = 0.25); **^{1}H NMR** (400 MHz, DMSO-d_6): δ_H = 8.68 (dd, *J* = 7.7, 1.6 Hz, 1H), 8.05 (dd, *J* = 7.9, 1.5 Hz, 1H), 7.87−7.83 (m, 2H), 7.81−7.72 (m, 2H), 7.66 (s, 1H), 7.62−7.54 (m, 3H), 3.97 (s, 3H), 3.89 (s, 3H) ppm; **^{13}C{^{1}H} NMR** (101 MHz, DMSO-d_6): δ_C = 164.7, 162.9, 144.1, 137.8, 137.8, 132.9, 130.5, 130.4, 130.1, 130.0, 129.0, 128.8, 128.6, 124.8, 122.8, 116.8, 108.3, 53.2, 53.2 ppm; **HRMS-ESI**(+) (*m*/*z*): calcd. for $C_{21}H_{17}N_2O_4$ [**M** + **H**]$^+$ 361.1182, found 361.1180.

*Diethyl 5-(3-chlorophenyl)pyrazolo[5,1-a]isoquinoline-1,2-dicarboxylate (**3s**).* Yellow solid (77 mg, yield 91%, mp 182−184 °C), (*n*-hexane/EtOAc = 2:1, R_f = 0.25); **^{1}H NMR** (300 MHz, $CDCl_3$): δ_H = 8.96−8.90 (m, 1H), 8.09 (d, *J* = 7.6 Hz, 1H), 7.82 (d, *J* = 6.4 Hz, 1H), 7.73−7.68 (m, 1H), 7.59−7.55 (m, 2H), 7.45 (brs, 1H), 7.31 (t, *J* = 7.3 Hz, 1H), 7.18 (brs, 1H), 4.48 (d, *J* = 7.1 Hz, 2H), 4.41 (t, *J* = 7.1 Hz, 2H), 1.44 (d, *J* = 7.1 Hz, 3H), 1.37(d, *J* = 7.1 Hz, 3H) ppm; **^{13}C{^{1}H} NMR** (75 MHz, $CDCl_3$): δ_C = 163.9, 162.5, 144.8, 137.9, 137.6, 132.3, 129.8, 129.2, 129.1, 129.0, 128.9, 128.2, 127.8, 127.5, 126.9, 125.0, 122.9, 115.5, 107.7, 61.2, 61.0, 13.7, 13.6 ppm; **HRMS-ESI**(+) (*m*/*z*): calcd. for $C_{23}H_{20}{}^{35}ClN_2O_4$ [**M** + **H**]$^+$ 423.1105, found 423.1111.

■ ASSOCIATED CONTENT

Data Availability Statement

The data underlying this study are available in the published article and its Supporting Information.

Supporting Information

The Supporting Information is available free of charge at https://pubs.acs.org/doi/10.1021/acsomega.4c11109.

General experimental procedures; computational details; characterization details; and ^{1}H NMR, ^{13}C NMR, and HRMS spectra of all compounds (PDF)

Accession Codes

CCDC 2401250 (compound **3r**) contains the supplementary crystallographic data for this paper. These data can be obtained free of charge from The Cambridge Crystallographic Data Centre via www.ccdc.cam.ac.uk/structures.

■ AUTHOR INFORMATION

Corresponding Author

Saeed Balalaie − *Peptide Chemistry Research Institute, K. N. Toosi University of Technology, Tehran, Iran;* orcid.org/0000-0002-5764-0442; Phone: +98-21-23064226; Email: Balalaie@kntu.ac.ir; Fax: +98-21-22889403

Authors

Fatemeh Abdiyan Mobarakeh − *Peptide Chemistry Research Institute, K. N. Toosi University of Technology, Tehran, Iran*

Mohammad Rezaei-Gohar − *Peptide Chemistry Research Institute, K. N. Toosi University of Technology, Tehran, Iran*

Kamran Amiri − *Peptide Chemistry Research Institute, K. N. Toosi University of Technology, Tehran, Iran;* orcid.org/0000-0001-5455-4832

Hamid Reza Bijanzadeh − *Department of Environmental Sciences, Faculty of Natural Resources and Marine Sciences, Tarbiat Modares University, Noor, Iran*

Frank Rominger − *Organisch-Chemisches Institut der Universität Heidelberg, 69120 Heidelberg, Germany*

Complete contact information is available at: https://pubs.acs.org/10.1021/acsomega.4c11109

Notes

The authors declare no competing financial interest.

■ ACKNOWLEDGMENTS

The authors thank Iran National Science Foundation (INSF, Grant 4027190) for the financial Support. S.B. thanks the Alexander von Humboldt Foundation for the research fellowship.

■ REFERENCES

(1) (a) Carey, J. S.; Laffan, L.; Thompson, C.; Williams, M. T. *Org. Biomol. Chem.* **2006**, *4*, 2337. (b) Laird, T. *Org. Process Res. Dev.* **2006**, *10*, 851.

(2) (a) Ding, S.; Yan, Y.; Jiao, N. Copper-catalyzed direct oxidative annulation of N-iminopyridinium ylides with terminal alkynes using O_2 as oxidant. *Chem. Commun.* **2013**, *49*, 4250−4252. (b) Lei, Y.; Xing, J.-J.; Xu, Q.; Shi, M. Synthesis of 5, 6-Dihydropyrazolo [5, 1-a] isoquinoline and Ethyl (Z)-3-Acetoxy-3-tosylpent-4-enoate through Tertiary-Amine-Catalyzed [3+ 2] Annulation. *Eur. J. Org. Chem.* **2016**, *2016*, 3486−3490. (c) Mousseau, J. J.; Bull, J. A.; Charette, A. B. Copper-catalyzed direct alkenylation of N-iminopyridinium ylides. *Angew. Chem., Int. Ed.* **2010**, *49*, 1115−1118. (d) Xiao, Q.; Ling, L.; Ye, F.; Tan, R.; Tian, L.; Zhang, Y.; Li, Y.; Wang, J. Copper-catalyzed direct ortho-alkylation of N-iminopyridinium ylides with N-tosylhydrazones. *J. Org. Chem.* **2013**, *78*, 3879−3885.

(3) (a) Qiu, G.; Kuang, Y.; Wu, J. N-Imide Ylide-Based Reactions: C-H Functionalization, Nucleophilic Addition and Cycloaddition. *Adv. Synth. Catal.* **2014**, *356*, 3483−3504. (b) Li, X.; Zhang, R.; Qi, Y.; Zhao, Q.; Yao, T. Rhodium (III)-Catalyzed C–H Activation/Annulation of N-Iminopyridinium Ylides with Alkynes and Diazo Compounds. *Org. Chem. Front.* **2021**, *8*, 1190−1196. (c) Dai, W.; Li, C.; Liu, Y.; Han, X.; Li, X.; Chen, K.; Liu, H. Palladium-Catalyzed [4+ 3] Dearomatizing Cycloaddition Reaction of N-Iminoquinolinium Ylides. *Org. Chem. Front.* **2020**, *7*, 2612−2617. (d) Yang, S.; Li, K.; Tang, Y.; Zheng, B.; Wang, W.; Wu, Y.; Xiao, Y.; Guo, H. Palladium-Catalyzed (5+ 3) Annulation of 4-Vinyl-4-Butyrolactones with C, N-Cyclic Azomethine Imines: Construction of Eight-Membered Ring. *Adv. Synth. Catal.* **2022**, *364*, 3967−3972.

(4) Wu, P.; Zhang, Y.; Cheng, Y. Sequential Ag (I) salt and chiral N-Heterocyclic carbene catalysis enables enantioselective and diastereoselective construction of complex heterocyclic molecules and the switch of stereoselectivity. *J. Org. Chem.* **2022**, *87*, 2779−2796.

(5) Shi, X.; Wang, Q.; Tang, Z.; Huang, H.; Cao, T.; Cao, H.; Liu, X. Divergent Synthesis of F-and CF3-Containing N-Fused Heterocycles Enabled by Fragmentation Cycloaddition of β-CF3−1, 3-Enynes with N-Aminopyridiniums Ylides. *Org. Lett.* **2024**, *26*, 1255−1260.

(6) Dugger, R. W.; Ragan, J. A.; Ripin, D. H. B. Survey of GMP bulk reactions run in a research facility between 1985 and 2002. *Org. Process Res. Dev.* **2005**, *9*, 253−258.

(7) (a) Koehn, F. E.; McConnell, O. J.; Longley, R. E.; Sennett, S. H.; Reed, J. K. Analogs of the marine immunosuppressant microcolin A: Preparation and biological activity. *J. Med. Chem.* **1994**, *37*, 3181−3186. (b) Zhou, H.; Bai, L.; Xu, R.; Zhao, Y.; Chen, J.; McEachern, D.; Chinnaswamy, K.; Wen, B.; Dai, L.; Kumar, P.; et al. Structure-based discovery of SD-36 as a potent, selective, and efficacious PROTAC degrader of STAT3 protein. *J. Med. Chem.* **2019**, *62*, 11280−11300. (c) Marco-Contelles, J.; do Carmo Carreiras, M.; Rodriguez, C.; Villarroya, M.; Garcia, A. G. Synthesis and pharmacology of galantamine. *Chem. Rev.* **2006**, *106*, 116−133.

(8) (a) Dore, A.; Asproni, B.; Scampuddu, A.; Gessi, S.; Murineddu, G.; Cichero, E.; Fossa, P.; Merighi, S.; Bencivenni, S.; Pinna, G. A. Synthesis, molecular modeling and SAR study of novel pyrazolo[5,1-f] [1,6]naphthyridines as CB2 receptor antagonists /inverse agonists. *Bioorg. Med. Chem.* **2016**, *24*, 5291−5301. (b) Löber, S.; Hübner, H.; Gmeiner, P. Fused azaindole derivatives: molecular design, synthesis and In vitro pharmacology leading to the preferential dopamine D3 receptor agonist FAUC 725. *Bioorg. Med. Chem. Lett.* **2002**, *12*, 2377−2380. (c) Xiong, Y.; Ullman, B.; Choi, J.-S. K.; Cherrier, M.; Strah-Pleynet, S.; Decaire, M.; Feichtinger, K.; Frazer, J. M.; Yoon, W. H.; Whelan, K.; et al. Identification of fused bicyclic heterocycles as potent and selective 5-HT2A receptor antagonists for the treatment of insomnia. *Bioorg. Med. Chem. Lett.* **2012**, *22*, 1870−1873. (d) Kuroda, S.; Akahane, A.; Itani, H.; Nishimura, S.; Durkin, K.; Kinoshita, T.; Tenda, Y.; Sakane, K. Discovery of FR166124, a novel water-soluble pyrazolo-[1,5-α] pyridine adenosine A1 receptor antagonist. *Bioorg. Med. Chem. Lett.* **1999**, *9*, 1979−1984.

(9) Pan, X.; Wang, H.; Xia, H.-G.; Wu, J. An unexpected three-component reaction of 2-alkylenecyclobutanone and N′-(2-alkynyl-benzylidene) hydrazide with water. *RSC Adv.* **2015**, *5*, 85225−85228.

(10) (a) Huang, P.; Yang, Q.; Chen, Z.; Ding, Q.; Xu, J.; Peng, Y. Metal cocatalyzed tandem alkynylative cyclization reaction of in situ formed N-iminoisoquinolinium ylides with bromoalkynes via C–H bond activation. *J. Org. Chem.* **2012**, *77*, 8092−8098. (b) Mousseau, J. J.; Bull, J. A.; Ladd, C. L.; Fortier, A.; Sustac Roman, D.; Charette, A. B. Synthesis of 2-and 2, 3-substituted pyrazolo [1, 5-a] pyridines: scope and mechanistic considerations of a domino direct alkynylation and cyclization of N-iminopyridinium ylides using alkenyl bromides, alkenyl iodides, and alkynes. *J. Org. Chem.* **2011**, *76*, 8243−8261.

(11) Shi, X.; Lin, Y.; Wei, J.; Zhao, L.; Guo, P.; Cao, H.; Liu, X. One-step synthesis of cyanated pyrazolo [1, 5-a] pyridines utilizing N-aminopyridines as a 1, 3-dipole and a nitrogen source. *Org. Chem. Front.* **2023**, *10*, 2892−2897.

(12) Guo, C.; Fleige, M.; Janssen-Müller, D.; Daniliuc, C. G.; Glorius, F. Switchable selectivity in an NHC-catalysed dearomatizing annulation reaction. *Nat. Chem.* **2015**, *7*, 842−847.

(13) (a) Le, K. K. A.; Nguyen, H.; Daugulis, O. 1-Aminopyridinium Ylides as Monodentate Directing Groups for sp3 C-H Bond Functionalization. *J. Am. Chem. Soc.* **2019**, *141*, 14728−14735. (b) Zhang, P.; Zhou, Y.; Han, X.; Xu, J.; Liu, H. N-heterocyclic carbene catalyzed enantioselective [3+ 2] dearomatizing annulation of saturated carboxylic esters with N-iminoisoquinolinium ylides. *J. Org. Chem.* **2018**, *83*, 3879−3888. (c) Zhao, J.; Wu, C.; Li, P.; Ai, W.; Chen, H.; Wang, C.; Larock, R. C.; Shi, F. Synthesis of pyrido [1, 2-b] indazoles via aryne [3+ 2] cycloaddition with N-tosylpyridinium Imides. *J. Org. Chem.* **2011**, *76*, 6837−6843. (d) Khosravi, H.; Ghazvini, H. J.; Kamangar, M.; Rominger, F.; Balalaie, S. Migratory Cycloisomerization of 1, 3-Dien-5-Ynes Conjugated with Pseudopeptides in Assembly of Benzo [7] Annulenes. *Chem. Commun.* **2022**, *58*, 2164−2167. (e) Golmohammadi, F.; Balalaie, S.; Fathi Vavsari, V.; Anwar, M. U.; Al-Harrasi, A. Synthesis of Spiro-β-Lactam-Pyrroloquinolines as Fused Heterocyclic Scaffolds through Post-Transformation Reactions. *J. Org. Chem.* **2020**, *85*, 13141−13152.

(14) (a) Huang, P.; Yang, Q.; Chen, Z.; Ding, Q.; Xu, J.; Peng, Y. Metal Cocatalyzed Tandem Alkynylative Cyclization Reaction of in Situ Formed N-Iminoisoquinolinium Ylides with Bromoalkynes via C–H Bond Activation. *J. Org. Chem.* **2012**, *77*, 8092−8098. (b) Yao, L.; Yu, X.; Mo, C.; Wu, J. Synthesis of Pyrazolo [5, 1-a] Isoquinolines via Silver (i)–Rhodium (i) Cooperative Catalysis in the Reaction of N′-(2-Alkynylbenzylidene) Hydrazide with Cycloprop-2-Ene-1, 1-Dicarboxylate. *Org. Biomol. Chem.* **2012**, *10*, 9447−9451. (c) Xiao, Q.; Sheng, J.; Ding, Q.; Wu, J. Silver Triflate-Palladium Chloride Cooperative Catalysis in a Tandem Reaction for the Synthesis of H-Pyrazolo [5, 1-a] Isoquinolines. *Adv. Synth. Catal.* **2013**, *355*, 2321−2326.

https://doi.org/10.1021/acsomega.4c11109
ACS Omega 2025, 10, 14063−14074